JOURNAL OF MATERIALS SCIENCE 6 (1971) 332-341

An Evaluation of Rate-Controlling Obstacles for Low-Temperature Deformation of Zirconium

D. H. SASTRY, Y. V. R. K. PRASAD, K. I. VASU
Materials Research Group, Metallurgy Department, Indian Institute of Science, Bangalore, India

The low-temperature plastic flow of alpha-zirconium was studied by employing constant-rate tensile tests and differential-stress creep experiments. The activation parameters, enthalpy and area, have been obtained as a function of stress for pure, as well as commercial zirconium. The activation area is independent of grain size and purity and falls to about $9b^2$ at high stresses. The deformation mechanism below about 700 ° K is found to be controlled by a single thermally activated process, and not a two-stage activation mechanism. Several dislocation mechanisms are examined and it is concluded that overcoming the Peierls energy humps by the formation of kink pairs in a length of dislocation is the rate-controlling mechanism. The total energy needed to nucleate a double kink is about 0.8 eV in pure zirconium and 1 eV in commercial zirconium.

1. Introduction

A wealth of data is available on the deformation characteristics in fcc metals [1-6], while detailed investigations of a similar nature are lacking in cph metals, presumably because of the complexity introduced as a result of the variations in the axial ratio. Whereas it is generally thought that the low temperature plastic flow in magnesium [7, 8], zinc [9, 10] and cadmium [11, 12] is controlled by intersection of glide and forest dislocations, there is no general agreement as regards the mechanism of deformation in metals with an axial ratio less than ideal. Rapperport and Hartley [13] observed in zirconium a linear relation between ln τ and T in the range 77 to 1073° K, where τ is the shear flow stress and T, the absolute temperature. Tensile data between 300 and 773° K reported by Guard and Keeler [14] for "crystal bar" zirconium also conform well with the linear ln τ–T relationship. This is supported by more recent work on zirconium-oxygen alloys [15]. In contrast, Westlake [16] has shown that below room temperature $\tau^{2/3}$ varies linearly with $T^{2/3}$ for zirconium single crystals. Besides, some investigators [17, 18] have observed two rate-controlling dislocation processes to occur in succession in zirconium below 600° K while only a single thermally activated mechanism was reported in the work of Mills and Craig [19], Ramaswami and Craig [20] and Baldwin and Reed-Hill [15], before the deformation mechanism becomes athermal. The rate-controlling mechanism below 600° K has been attributed either to the interstitial atom-dislocation interaction or to the Peierls-Nabarro force.

In the present work, the low temperature deformation mechanism in alpha zirconium has been studied with a view to gathering additional information which may throw light on the operative mechanism(s). Constant rate tensile tests and differential stress creep experiments are employed to derive the activation energy and activation area characterising the obstacles to dislocation motion.

2. Experimental

Experiments were conducted on high-purity zirconium and commercial grade zirconium. Their analyses are included in table I. Commercial zirconium was rolled into sheets, and specimens for tensile and creep tests were machined with their axes in the rolling direction. The specimens employed had an approximate thickness of 0.5 mm. Pure zirconium was tested in the form of wires of about 1 mm diameter. All specimens were annealed at 1073° K for 30 min in a dynamic vacuum of better than 5×10^{-6}

TABLE I Analysis of zirconium.

Impurity	Concentration in ppm	
	Pure zirconium	Commercial zirconium (2.2% Hf)
Al	35	235
Si	—	135
Fe	90	125
Cr	—	95
Mn	—	20
Cu	—	25
Ti	42	25
Sn	—	25
W	—	50
Pb	—	70
O	—	1500
H	—	30
C	43	102
N	5	668
Others	10	110

torr. Different average grain diameters were obtained by controlling the mechanical treatment only. Each specimen was etched in a solution of 46% HNO_3, 8% HF and 46% H_2O before testing.

Tensile testing was done in a modified Hounsfield tensometer [12, 21] with provision for constant cross-head speeds. The load on the sample was recorded by measuring the deflection of the 2-Ton Spring beam with the help of an LVDT transducer, the amplified output of which is fed to a millivolt recorder. The sensitivity of the load measurement was 2.0 kg. The use of an extensometer fitted with an LVDT coil permitted recording of elongation on the gauge length (2.5 cm) of the sample. The sensitivity of the strain measurement was 5×10^{-4}. Tensile testing in the range of 87 to 900° K was carried out on commercial zirconium employing three tensile strain rates of 7.8×10^{-4}, 1.8×10^{-4} and 2.1×10^{-5} sec^{-1}, and on pure zirconium employing two tensile strain rates of 7.8×10^{-4} and 1.8×10^{-4} sec^{-1}. For testing at 87, 197 and 300° K, the sample, fixed in a cage, was immersed in liquid oxygen, dry ice plus alcohol, and stirred water respectively. In the range of 300 to 600° K, a thermostatically controlled paraffin oil/silicone oil bath was used, while for higher temperatures a resistance wound furnace with provision for maintenance of an inert (purified argon) atmosphere was employed. Tensile samples had an average grain diameter of 0.005 mm for commercial zirconium and 0.01 mm for pure zirconium.

Creep experiments were conducted on a constant stress tensile creep unit [21] in which the applied stress is maintained constant during the test with the help of a smooth contour. The creep elongation was measured using an LVDT transducer together with an amplifier and a millivolt recorder. The accuracy of the strain measurement was 10^{-5}. Creep testing on commercial zirconium was done on samples with a variety of grain sizes at 87, 197 and 300° K while the tests were conducted only at 87° K on pure zirconium (average grain diameter = 0.01 mm). The general procedure was as follows: The sample, kept at the required temperature, was loaded in small steps until creep was observed on the recorder chart. Then a small incremental load was added and the incremental creep curve recorded. The incremenal load was then removed to record the decremental creep curve. The procedure was repeated until the creep rate became too low to be recorded accurately. At this stage a major load was added and the process of small stress addition and removal was repeated. With this procedure, it was possible to study the change in the creep rate following increments and decrements of stress at different stress levels.

3. Results

The variation of tensile flow stress, σ, with temperature and strain rate, $\dot{\epsilon}$, for zirconium of two purities is presented in fig. 1. All the flow stress values reported were measured at 0.1%

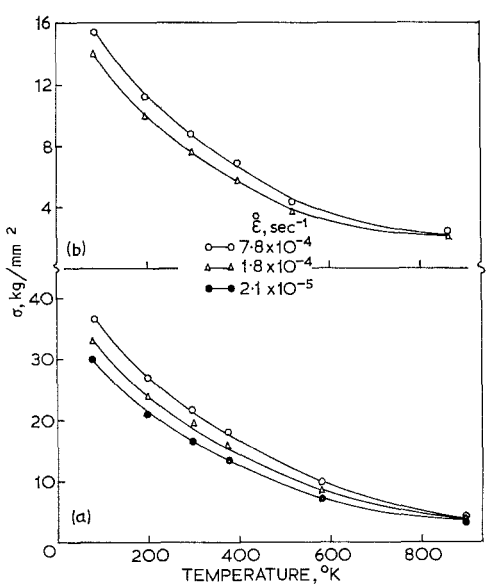

Figure 1 Effect of temperature and strain rate on the flow stress of (a) commercial zirconium and (b) pure zirconium.

offset from the modulus line and are unaccounted for the variation of shear modulus with temperature. The flow stress has reached a constant value, almost independent of strain rate, at about 900° K, both for commercial zirconium and pure zirconium.

Seeger [2] considered the flow shear stress, τ, to consist of two components as:

$$\tau = \tau_\mu + \tau^* \quad (1)$$

where τ_μ is the stress required to overcome the long-range stress fields of dislocations and other athermal obstacles and τ^* is the temperature and strain-rate dependent stress controlled by short-range obstacles. The effective shear stress, τ^*, at any temperature is obtained from

$$\tau^* = \tfrac{1}{2}(\sigma - \sigma_{900})$$

where σ is the tensile flow stress at the temperature T and σ_{900} is the flow stress at 900° K. The variation of the thermal component of the flow stress with temperature and strain rate is documented in fig. 2. It is seen that τ^* is higher for

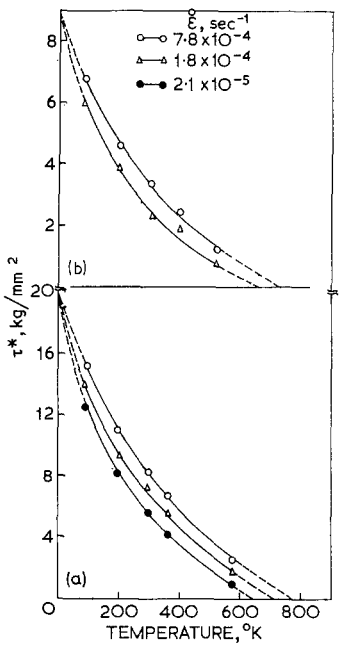

Figure 2 Variation of effective stress with temperature and strain rate for (a) commercial zirconium and (b) pure zirconium.

commercial zirconium than for pure zirconium at a given temperature and strain rate. It is also seen that the temperature, T_c, at which the thermal component of the flow stress vanishes, increases with strain rate in accordance with the theory of thermally activated flow [2]. At a given strain rate, T_c for commercial zirconium is higher than that for pure zirconium. The values of the critical temperature, T_c, are given in table II.

TABLE II Critical temperature as a function of strain rate for zirconium.

Strain rates $\dot{\epsilon}$, sec^{-1}	Critical temperature, T_c, °K	
	Commercial zirconium	Pure zirconium
7.8×10^{-4}	780	730
1.8×10^{-4}	720	650
2.1×10^{-5}	640	—

The rate-controlling obstacles are usually identified by measuring the activation enthalpy, H, and the activation area, A. Conrad and Wiedersich [22] and subsequently Li [23] derived expressions, without assuming any specific dislocation mechanism, for the evaluation of the activation enthalpy from experimental data. The expression of Li is:

$$H = -k\left[\frac{\delta \ln(\dot{\gamma})}{\delta(1/T)}\right]_{\tau}^{*} = -k\left[\frac{\delta \ln \dot{\epsilon}}{\delta(1/T)}\right]_{\tau}^{*} \quad (2)$$

where $\dot{\gamma}$ is the shear strain rate and k, the Boltzmann's constant. With the help of equation 2, the thermal activation enthalpy can be calculated at any stress from the data of fig. 2. The dependency of H on τ^* can thus be obtained This procedure, of course, assumes that the structure is identical for the different specimens used. This is a justifiable assumption inasmuch as the flow stress values were measured at a constant strain and H was calculated at a given stress. The variation of H with stress is shown in fig. 3a for commercial zirconium. Again, by reading the temperature corresponding to the stress in fig. 2, the variation of H with temperature can be obtained; this variation for commercial zirconium is as shown in fig. 3b. The corresponding data for pure zirconium are documented in fig. 4. Figs. 3b and 4b suggest that the activation enthalpy varies linearly with temperature as is to be expected from the equation:

$$H = kT \ln(P/\dot{\gamma}) \quad (3)$$

where P is a frequency factor.

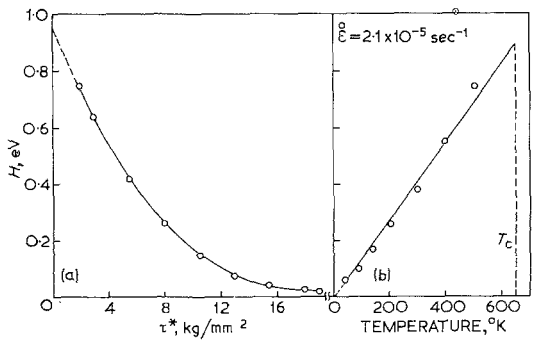

Figure 3 Variation of activation enthalpy with (a) effective stress and (b) temperature for commercial zirconium.

The total enthalpy, H_0, required for the thermal activation process was arrived at in the following ways: (i) extrapolation of the H-τ^* curve to $\tau^* = 0$ (ii) extrapolation of the H-T plot to $T = T_c$ and (iii) knowing T_c at two strain rates and using the equation:

$$\frac{\dot{\gamma}_2}{\dot{\gamma}_1} = \frac{\dot{\epsilon}_2}{\dot{\epsilon}_1} = \frac{\exp(-H_0/kT_{c2})}{\exp(-H_0/kT_{c1})} \qquad (4)$$

The data given in table II were used for the evaluation of H_0 from the strain-rate dependence of T_c. The values of H_0 calculated by the above three methods are recorded in table III. Commercial zirconium gives consistently higher values of H_0 compared with pure zirconium.

TABLE III Total activation enthalpy for low temperature deformation of zirconium.

Metal	Total activation enthalpy, H_0, eV			Average H_0 eV
	H vs. τ^*	H vs. T	Effect of $\dot{\gamma}$ on T_c	
Commercial Zr	0.95	0.90	1.06	0.97
Pure Zr	0.83	0.75	0.74	0.78

Results on differential-stress creep experiments were utilised to calculate the activation areas in zirconium. Commercial zirconium exhibited logarithmic creep at the three temperatures and in the stress ranges given below.

Temp. (°K)	Stress range used (kg/cm²)
87	1920 to 7245
197	1200 to 4025
300	900 to 3565

Pure zirconium, likewise, exhibited logarithmic creep at 87° K in the stress range of 1100 to 4000 kg/cm². Graphical differentiation of the creep strain – log time plots yielded the creep rate, $\dot{\epsilon}$, which is shown in fig. 5 as a function of creep strain to indicate the effect of repeated stress increments and decrements. An evaluation

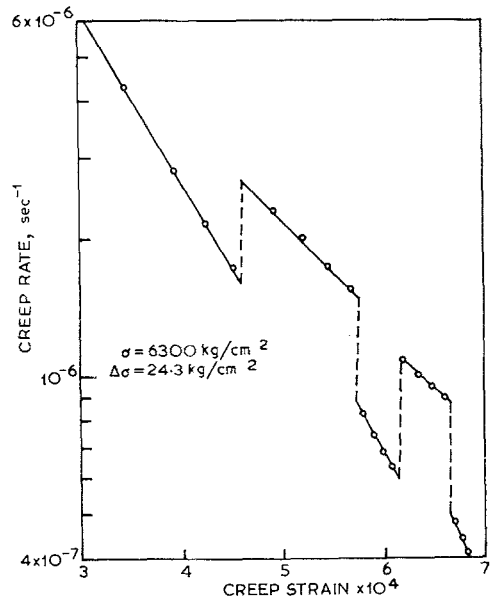

Figure 5 Effect of small repeated stress changes on the creep rate of commercial zirconium at (a) 87° K and (b) 300° K.

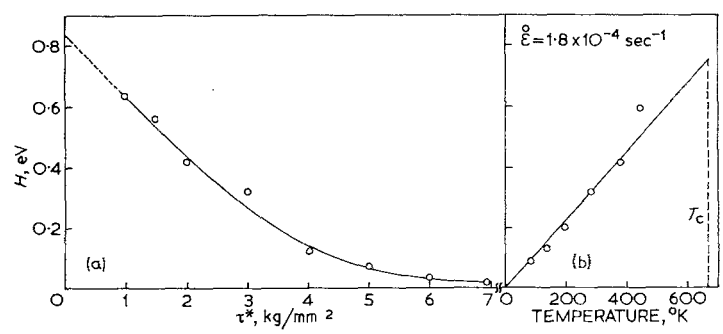

Figure 4 Variation of activation enthalpy with (a) effective stress and (b) temperature for pure zirconium.

[23] of the activation area is made using the equation

$$A = \frac{kT}{\mathbf{b}} \left[\frac{\Delta \ln \dot{\gamma}}{\Delta \tau^*}\right]_T = \frac{2kT}{\mathbf{b}} \left[\frac{\Delta \ln \dot{\epsilon}}{\Delta \sigma}\right]_T \quad (5)$$

where **b** is the Burgers vector. The activation area is also obtained from the $H - \tau^*$ curves in figs. 3 and 4 since

$$A = -(1/\mathbf{b})(\delta H/\delta \tau^*) \quad (5a)$$

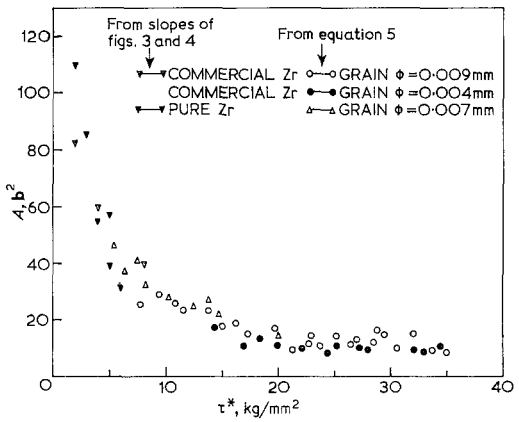

Figure 6 Dependence of activation area on effective stress for zirconium at 87° K.

The dependence of activation area on effective stress at 87° K is presented in fig. 6 for zirconium of the two purities. Fig. 6 makes evident the following points:

(i) the activation area in commercial zirconium is independent of grain size,

(ii) the activation area in commercial zirconium is almost the same as that in pure zirconium at a given effective stress,

(iii) the activation areas obtained from equation 5a using the slopes of figs. 3 and 4 compare well with those from creep data,

(iv) the activation area in both the materials used decreases from about 100 $\mathbf{b}^2$ at $\tau^* = 2$ kg/mm² to 9 $\mathbf{b}^2$ at $\tau^* = 35$ kg/mm².

The measured activation areas in commercial zirconium at 197 and 300° K are given in fig. 7. The results at 197° K again suggest that activation area is independent of grain size. The activation area has fallen at high effective stresses to about 15 $\mathbf{b}^2$ at 197° K and 22 $\mathbf{b}^2$ at 300° K.

4. Discussion

Soo and Higgins [17] and Das Gupta and Arunachalam [18] observed two stages of thermal activation below about 600° K in

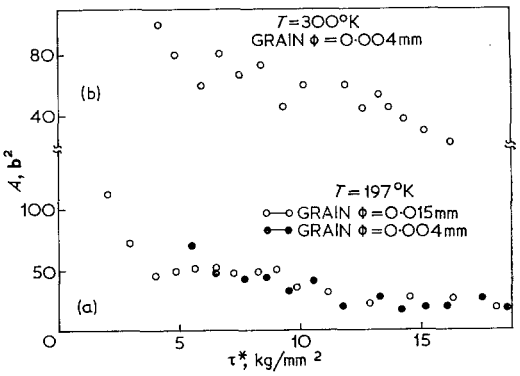

Figure 7 Variation of activation area with effective stress at (a) 197° K and (b) 300° K for commercial zirconium.

zirconium. The most direct manner of determining whether one or more rate-controlling mechanisms are operative would be to determine the variation of activation enthalpy as a function of effective stress. If the results would fit a single curve, then that would be a strong indication for only a single rate-controlling mechanism. The total activation enthalpy can be written [24, 25] as:

$$H_0 = H + \mathbf{b} \int_0^{\tau^*} A.\mathrm{d}\tau^* \quad (6)$$

H_0 was calculated as a function of stress from the experimental data in the following manner. The integral of equation 6 was solved graphically, by determining the area under the curve of fig. 6. Due to non-availability of activation area values at τ^* close to zero, the difference between H_0 (taken as 1 eV for commercial zirconium) and H taken at a small effective stress of 3 kg/mm² was set equal to the area under the $A - \tau^*$ curve up to that effective stress. In other words, it was assumed that H_0 does not change over this limited stress range. At larger values of τ^*, the area was measured directly and H_0 determined from equation 6. The results of this calculation for both pure and commercial zirconiums are shown in fig. 8, which indicates that H_0 is constant throughout and there is only one rate-controlling mechanism over the entire stress range studied. Supporting evidence for this conclusion is obtained from figs. 3b and 4b where it is seen that H is a linear function of temperature as required for a single thermally activated mechanism. Fig. 8 also yields average H_0 values of 1.08 eV for commercial zirconium and 0.85 eV for pure zirconium which are consistent with the data given in table III. Thus it may be

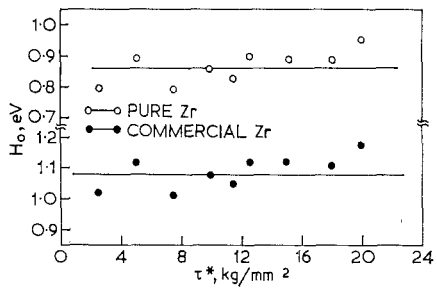

Figure 8 The variation of H_0 with effective stress for zirconium.

concluded that only one dislocation mechanism controls the flow stress in zirconium below about 700° K.

Regarding the rate-controlling mechanism for low temperature deformation of zirconium, five possibilities may be considered: (i) mutual intersection of glide and forest dislocations, (ii) overcoming the strain fields due to the presence of interstitial impurity atoms (i.e. Fleischer interaction), (iii) thermally activated depinning of dislocations from substitutional impurity atoms (i.e. Friedel model), (iv) cross slip of dislocations, and (v) overcoming the Peierls-Nabarro (*P-N*) stress. In the light of the experimental data presented above each one of the mechanisms will now be examined.

The intersection of glide dislocations with forest dislocations can readily be eliminated as the operative mechanism, since the experimental activation area is found to be very small, about $9\mathbf{b}^2$ (fig. 6). Such a small activation area requires the presence of a large dislocation density. The fact that the activation area is independent of grain size (fig. 6, 7) further disqualifies the intersection mechanism for, in cph metals, the activation area may also be a function of grain size if intersection were rate-controlling [10, 26].

Fleischer [27-29] proposed that the lowering of flow stress by an increase in temperature in somewhat impure metals can be understood in terms of an interstitial hardening model. The introduction of impurity atoms with a smaller size produces in the lattice both symmetrical and asymmetrical distortions. Asymmetrical distortions will have large interactions with both screw and edge dislocations and these are to be ovecome for plastic flow to occur. If the interstitial atoms act as barriers to the motion of dislocations, the variation of flow stress with temperature is given by:

$$\left[\frac{\tau^*}{\tau_0^*}\right]^{\frac{1}{2}} = 1 - \left[\frac{T}{T_c}\right]^{\frac{1}{2}} \tag{7}$$

where τ_0^* is the thermal component of flow stress at 0° K. Fig. 9a shows that the above relation is not obeyed satisfactorily either for commercial zirconium or for pure zirconium. The value of τ_0^* should, according to the theory of thermally activated deformation, remain the same at different strain rates. The datum points for commercial zirconium in fig. 9a do not appear to yield linear plots converging at $T = 0$. If one attempts to represent the data by straight lines, the critical temperature for commercial zirconium at a strain rate of 7.8×10^{-4} sec^{-1} turns out to be about 1200° K which is not compatible with either the present experimental data or the results of other workers [15-20]. Conrad [30] has alternately suggested that for thermally activated overcoming of interstitial atoms, the effect of stress on activation enthalpy is given by:

$$H = B(\tau_0^* - \tau^*)^2 \tag{8}$$

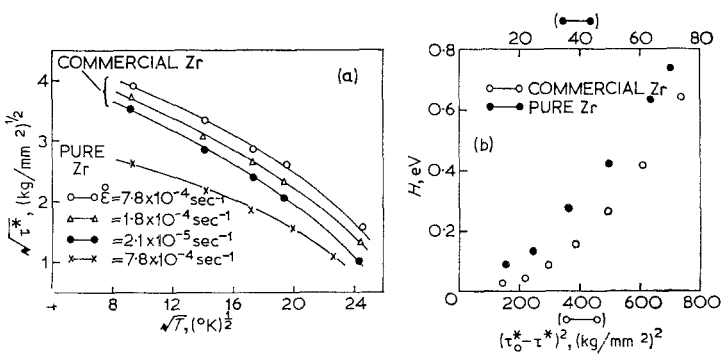

Figure 9 Plots to test the applicability of Fleischer's model to the deformation of zirconium.

where B is a constant. Fig. 9b shows that the variation of activation enthalpy for commercial zirconium is not in accordance with equation 8 either. Differentiation of equation 8 implies that the activation area varies linearly with stress, which is not the experimental finding (fig. 6).

Perhaps the most convincing evidence against the operation of Fleischer's model stems from the measured activation areas in zirconium of the two purities. The activation area for this model is directly proportional to the average distance between the interstitial atom stress centres, which is related to the concentration of interstitial impurities. The total interstitial impurity (O, H, C, N) contents in commercial zirconium and pure zirconium are 0.23% and 0.005% respectively (table I). Hence, the activation area at a given effective stress is expected to be about several times higher (the average distance between obstacles being inversely proportional to the square root of the concentration) in pure zirconium than in commercial zirconium. That this is not observed is clear from fig. 6. For instance, at $\tau^* = 10$ kg/mm^2, creep experiments on both the purities resulted in an activation area of about $30\mathbf{b}^2$. One experimental observation is, however, in agreement with Fleischer's model: the effective stress is a strong function of impurity content in the entire temperature range studied (fig. 2).

Substitutional solute atoms having a size difference will interact with the edge dislocations and can cause a "pinning" effect. Friedel [31, 32] assumes that the decrease in flow stress with temperature can be accounted for on the basis of a thermally activated depinning model and obtains the relation:

$$\tau^* = \tau_0^* \left[1 - \frac{T}{T_c}\right]^{3/2} \qquad (9)$$

The variation of the flow stress with temperature predicted by the Friedel's model can be tested by the plot of τ^* versus $[1 - T/T_c]^{3/2}$, knowing the critical temperature. This is done in fig. 10 for commercial zirconium using the data of critical temperature presented in table II. If a single straight line is drawn through the points, the standard deviation is more than what can be accounted for on the basis of experimental inaccuracies. Concentrating on data for $\dot{\epsilon} = 2.1 \times 10^{-5}$ sec^{-1}, a straight line such as the one shown in fig. 10 will yield a value of 15 kg/mm^2 for τ_0^* (when $T = 0$), which is less than that experimentally observed at 87° K for $\dot{\epsilon} = 7.8 \times 10^{-4}$ sec^{-1}. Thus equation 9 representing Friedel's depinning model is not valid for the present results on zirconium. Also, the activation area should be strongly dependent on the solute atom concentration for Friedel's model of dislocation unpinning. Despite the fact that the substitutional solute concentration is considerably different (2.29% in commercial zirconium and less than 0.02% in pure zirconium), the stress dependence of activation area is identical for the two impurity levels (fig. 6). Thus, it may be inferred that the temperature dependence of flow stress in zirconium is not accounted for by the thermally activated unpinning of dislocations from randomly distributed solute atoms.

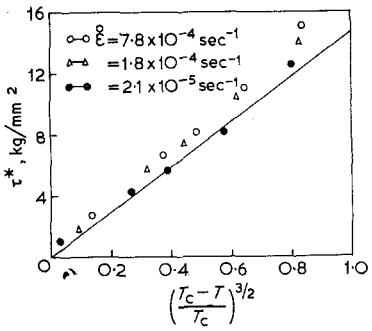

Figure 10 Plot to test the applicability of Friedel's model to the experimental data on the temperature variation of effective stress of commercial zirconium.

Another mechanism which can yield an activation area of the order experimentally obtained is the thermally activated cross slip. When dislocations on a prism plane assume a screw orientation, they can dissociate into a pair of partials on the basal plane separated by a stacking fault. Continued slip on the prismatic planes then requires recombination of the partials and cross slipping back onto the prism plane. Flynn *et al* [33] and Dorn [34] have shown that if the cross slip mechanism is rate-controlling the following relationship should be obeyed:

$$\frac{1}{\tau^* T} = R_1 - \frac{R_2}{T} \qquad (10)$$

where R_1 and R_2 are constants. The results recorded in fig. 11 show that $1/\tau^* T$ does not decrease linearly with $1/T$ over the temperature range of thermal activation. The above equation is expected to be valid only when τ^* on the basal plane is zero and τ^* on the prismatic plane is small [35]. The operation of the cross slip

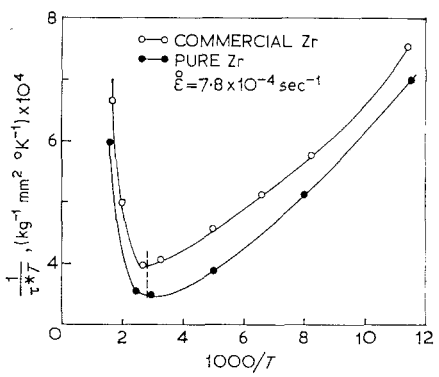

Figure 11 Effect of temperature on the flow stress of zirconium to examine the mechanism of cross slip.

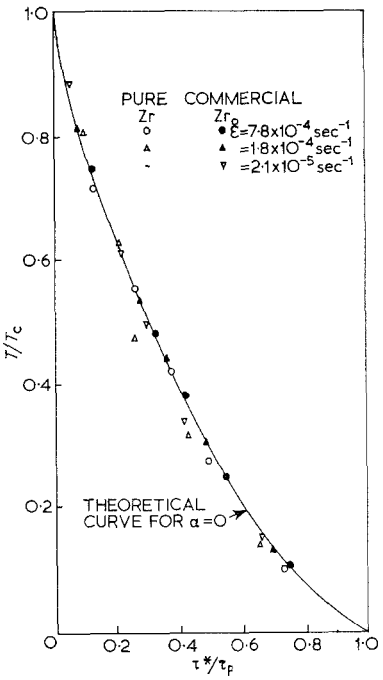

Figure 12 Effective stress as a function of temperature in dimensionless units for zirconium.

mechanism below 370° K where τ^* is large is not likely.

The rate-controlling mechanisms for low-temperature deformation of zirconium may then be associated with the Peierls-Nabarro force, because this mechanism is characterised by a strong temperature-dependence of flow stress and small activation area. The Peierls mechanism has been discussed by Seeger [36], Seeger *et al* [37], Weertman [38], Lothe and Hirth [39], Seeger and Schiller [40], Friedel [32], Dorn and Rajnak [41] and Guyot and Dorn [42]. For the present case, the theory of Dorn and Rajnak [41] will be adopted. Assuming a line energy model for the movement of a dislocation line from one potential valley to the next over the Peierls hill, Dorn and Rajnak calculated the stress-dependence of the activation enthalpy, H_n, required to nucleate a pair of kinks, by the lateral separation of which the dislocation line is carried forward by an atomic spacing. At the critical temperature, the total energy for kink nucleation is supplied by a thermal fluctuation and hence

$$(H_n)_{Tc} = 2H_k$$

where H_k is the energy of a single kink. The ratio τ^*/τ_p, where τ_p is the Peierls stress (equal to τ_0^*), has been theoretically deduced as a function of T/T_c and is shown in fig. 12 as the solid curve for the perturbation factor $\alpha = 0$ (α varies between -1 and $+1$ and perturbs the shape of the Peierls' hill from the purely sinusoidal variation that is obtained at $\alpha = 0$). Using the critical temperatures in table II and the extrapolated value of τ^* at 0° K for τ_p, the flow stress variation with temperature for commercial zirconium is shown in the same figure for the three strain rates employed. It is seen that the data fit well with the universal theoretical curve for $\alpha = 0$. Similarly, a good fit (fig. 12) with the theory of Dorn and Rajnak is obtained when the flow stress variation with temperature for pure zirconium is considered.

An essential characteristic of the Peierls mechanism is the small activation area, about $10\mathbf{b}^2$, which is, in fact, experimentally observed (fig. 6). The expected variation of activation area for the double kink mechanism [41] with τ^*/τ_p is shown in fig. 13. Values of $(\tau_p/2H_k)A\mathbf{b}$ were calculated using the measured activation areas, the Peierls stress and the value of H at $T = T_c$. These data points are also shown in fig. 13. There is good agreement between the experimental and theoretical values, except at low stresses, where the experimentally determined values of A increase rapidly because athermal mechanisms begin to operate here.

For the Peierls mechanism, the strain rate is given by:

$$\dot{\epsilon} = \tfrac{1}{2}\rho a\mathbf{b}\nu_0 \frac{L}{w} \exp(-2H_k/kT_c) \qquad (11)$$

where a = distance between adjacent Peierls valleys, L = the mean length swept out by a pair

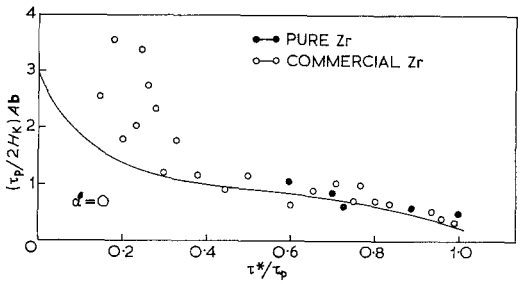

Figure 13 Activation area in zirconium as a function of effective stress in dimensionless units.

of kinks once nucleation occurs in that length, w = critical width of a pair of kinks at the saddle point free energy configuration, and ν_0 = the Debye frequency. By substituting appropriate values for H_k, T_c and $\dot{\epsilon}$ and taking $a = \mathbf{b} = 3.2$Å (lattice parameter) and $w = 50\mathbf{b}$, a value of 100 cm^{-1} is obtained for ρL in commercial zirconium, which is of the expected order of magnitude. Further, the values of the function

$$\frac{2H_k\pi}{aU} \Big/ \left[\frac{\tau_p a\mathbf{b}}{\pi U}\right]^{\frac{1}{2}},$$

where U is the line energy of a dislocation, have been calculated by Dorn and Mitchell [35]; for $\alpha = 0$ the function is 5.7. Using this value and the values of H_k and τ_p for commercial zirconium the line energy of a dislocation is calculated to be 5×10^8 eV/cm which compared well with the generally accepted value of $\mu\mathbf{b}^2/2$ where μ is the shear modulus.

It is seen that introduction of impurities in pure zirconium shifts T_c to higher temperatures (table II) and also increases the total activation enthalpy (table III), H_0, i.e. the energy needed to nucleate a pair of kinks. This means that stronger obstacles are present in commercial zirconium. The Peierls barrier will then be higher and the Peierls stress should increase. This, in fact, is qualitatively the case (fig. 2). However, whereas there is an increase of only 25% in the value of $2H_k$ (from 0.78 to 0.97 eV) there is a 100% increase in the value of Peierls stress from highly pure to commercial zirconium. As the theoretical value of τ_p is directly related [43] to the shear modulus, there should be a corresponding increase in μ from pure to commercial zirconium. Though a 100% change in shear modulus is not commonly observed, this enormous increase in Peierls stress can be qualitatively understood. Long-range ordering of oxygen atoms has been reported [44] in zirconium-oxygen alloys containing about 26 at. % oxygen. The oxygen atoms are supposed to occupy octahedral sites in the zirconium crystal structure. Hence, short range ordering may occur in alloys with low oxygen concentration. The movement of dislocations through the crystal will then disturb the minimum energy arrangement of oxygen atoms. This requires work and may be revealed in the form of increased flow stress at 0° K. This explanation for the increase in Peierls stress looks plausible: commercial zirconium contains as much as 1500 ppm of oxygen while pure zirconium contains practically none (table I); hence the observed increase in Peierls stress. Thus, it may be stated that the low temperature deformation in zirconium appears to be controlled by the Dorn-Rajnak formulation of the Peierls mechanism.

5. Summary

(i) Constant strain rate tests in the range of 87 to 900° K indicated that the deformation of zirconium below about 700° K is controlled by a single thermally activated mechanism. The critical temperature increased with strain rate.
(ii) Alpha zirconium exhibited logarithmic creep at temperatures between 87 and 300° K over a wide stress range. Results on differential-stress creep experiments were utilised to calculate the activation area.
(iii) The activation area in zirconium was observed to be independent of grain size and its impurity content.
(iv) Activation area was a decreasing function of stress, falling to about $9\mathbf{b}^2$ at high effective stresses at 87° K.
(v) A comparison of these results with several dislocation mechanisms of current interest showed best agreement with the Dorn-Rajnak model for the nucleation of a double kink in a segment of dislocation to overcome the Peierls energy barriers.
(vi) The energy needed to nucleate a pair of kinks was calculated to be about 1 eV in commercial zirconium and 0.8 eV in pure zirconium.
(vii) The high increase in Peierls stress in commercial zirconium could only be qualitatively explained on the basis of short-range ordering of oxygen atoms.

Acknowledgement

The authors are thankful to Dr S. Dhawan, Director, Indian Institute of Science, for his

interest in the work and to other members of the Materials Research Group for their co-operation.

References

1. Z. S. BASINSKI, *Phil. Mag.* **4** (1959) 393.
2. A. SEEGER, "Dislocations and Mechanical Properties of Crystals" (John Wiley: New York 1957) p. 243.
3. S. K. MITRA, P. W. OSBORNE, and J. E. DORN, *Trans. AIME* **221** (1961) 1206.
4. S. K. MITRA and J. E. DORN, *ibid* **226** (1963) 1015.
5. H. CONRAD, "High Strength Materials" (John Wiley: New York, 1965) p. 436.
6. K. R. EVANS and W. F. FLANAGAN, *Phil. Mag.* **17** (1968) 535.
7. H. CONRAD, L. HAYS, G. SCHOECK, and H. WIEDERSICH, *Acta Metallurgica* **9** (1961) 367.
8. Z. S. BASINSKI, *Austral. J. Phys.* **13** (1960) 284.
9. P. LUKAC, *Z. Metallk.* **57** (1966) 559.
10. D. H. SASTRY, Y. V. R. K. PRASAD, and K. I. VASU, *Met. Trans.* **1** (1970) 1827.
11. P. LUKAC and Z. TROJANOVA, *Z. Metallk.* **58** (1967) 57.
12. D. H. SASTRY, Y. V. R. K. PRASAD, and K. I. VASU, *Acta Metallurgica* **17** (1969) 1453.
13. E. J. RAPPERPORT and C. S. HARTLEY, *Trans. AIME* **218** (1960) 869.
14. R. W. GUARD and J. H. KEELER, *Trans. ASM* **49** (1957) 449.
15. D. H. BALDWIN and R. E. REED-HILL, *Trans. AIME* **242** (1968) 661.
16. D. G. WESTLAKE, *ibid* **223** (1965) 368.
17. P. SOO and G. T. HIGGINS, *Acta Metallurgica* **16** (1968) 177, 187.
18. P. DAS GUPTA and V. S. ARUNACHALAM, *J. Mater. Sci.* **3** (1968) 271.
19. D. MILLS and G. B. CRAIG, *Trans. AIME* **242** (1968) 1881.
20. B. RAMASWAMI and G. B. CRAIG, *ibid* **239** (1967) 1226.
21. Y. V. R. K. PRASAD, D. H. SASTRY, and K. I. VASU, *J. Ind. Inst. Sci.* **51** (1969) 377.
22. H. CONRAD and H. WIEDERSICH, *Acta Metallurgica* **8** (1960) 128.
23. J. C. M. LI, "Dislocation Dynamics" (McGraw-Hill: New York, 1968) p. 87.
24. G. B. GIBBS, *Phys. Stat. Solidi* **10** (1965) 507.
25. R. J. ARSENAULT, *Acta Metallurica* **14** (1966) 831.
26. N. R. RISEBROUGH and E. TEGHTSOONIAN, *Canad. J. Phys.* **45** (1967) 591.
27. R. L. FLEISCHER, *Acta Metallurgica* **10** (1962) 835.
28. *Idem, J. Appl. Phys.* **33** (1962) 3504.
29. R. L. FLEISCHER and W. R. HIBBARD, "Relation between the Structure and Mechanical Properties of Metals" (HMSO: London, 1963) p. 261.
30. H. CONRAD, *Canad. J. Phys.* **45** (1967) 581.
31. J. FRIEDEL, "Dislocations" (Pergamon Press: New York and London, 1964) p. 379.
32. J. FRIEDEL, "Electron Microscopy and Strength of Crystals" (John Wiley: New York and London 1963) p. 605.
33. P. W. FLYNN, J. D. MOTE, and J. E. DORN, *Trans. AIME* **221** (1961) 1148.
34. J. E. DORN, "Energetics in Dislocation Mechanics" UCRL-10455, (1963).
35. J. E. DORN and J. B. MITCHELL, "High Strength Materials" (John Wiley: New York and London 1965) p. 510.
36. A. SEEGER, *Phil. Mag.* **1** (1956) 651.
37. A. SEEGER, H. DONTH, and F. PFAFF, *Discuss. Faraday Soc.* **23** (1957) 19.
38. J. WEERTMAN, *Phys. Rev.* **101** (1956) 1429.
39. J. LOTHE and J. P. HIRTH, *Phys. Rev.* **115** (1959) 543.
40. A. SEEGER and P. SCHILLER, *Acta Metallurgica* **10** (1962) 348.
41. J. E. DORN and S. RAJNAK, *Trans. AIME* **230** (1964) 1052.
42. P. GUYOT and J. E. DORN, *Canad. J. Phys.* **45** (1967) 983.
43. J. WEERTMAN and J. R. WEERTMAN, "Elementary Dislocation Theory" (Macmillan: New York, 1964) p. 159.
44. B. HOLMBERG and T. DAGERHAMN, *Acta. Chem. Scand.* **15** (1961) 919.

Received 28 August and accepted 24 November 1970.